JOURNAL OF COMPUTATIONAL PHYSICS 39, 112–127 (1981)

Shape Instabilities and Pattern Formation in Solidification: A New Method for Numerical Solution of the Moving Boundary Problem

JEFFREY B. SMITH

Department of Physics and Center for the Joining of Materials, Carnegie–Mellon University, Pittsburgh, Pennsylvania 15213

Received August 8, 1979; revised February 28, 1980

When a solidification front is advancing into a region of supercooled liquid, its shape is subject to instabilities which can lead to complex modes of growth. The evaluation of the growth pattern is determined by the interaction of the driving force of the instability due to heat diffusion with the restabilizing force due to surface tension, and its full development is a highly nonlinear process. A new method for solving the two-phase heat diffusion problem under these conditions is described. The method is based on a single-domain treatment (weak formulation) of the moving boundary problem, with the temperature field near the interface approximated by a piecewise linear function in the spirit of the finite-element technique. Calculated results for a model problem are in excellent agreement with the predictions of an analytical approximation.

I. INTRODUCTION

Dendritic crystal growth is a long-known but poorly understood phenomenon which has begun to receive renewed attention from physicists [1]. It has enormous practical importance in metallurgy, and it is also a fascinating example of the self-organizing of complex patterns within a simple physical system. While the essentials of the physics of solidification appear to be known, the process of pattern-generation presents challenges to understanding similar to those encountered in the study of hydrodynamic instabilities. The linear stability analysis of Mullens and Sekerka demonstrated that the patterns originate in an instability of the shape of the growing solid [2]. Recent work by Langer and Müller-Krumbhaar has included nonlinear effects, but only for small deviations from the steady-state shape of the interface [3]. Even in this regime a sophisticated combination of analytic and numerical techniques was required. The full development of the growth pattern is highly nonlinear, however, and methods are needed for the direct numerical solution of the solidification equations in the presence of the interface instability. This paper is, to my knowledge, the first report of such a method.

The following model of solidification in a pure material is used. The system

0021-9991/81/010112-16$02.00/0

consists of a finite two-dimensional region containing both solid and liquid. Heat transport in each phase is governed by a diffusion equation

$$\frac{\partial U}{\partial t} = D_i \nabla^2 U, \tag{1}$$

where $D_i = D_S$ or D_L is the thermal diffusivity and $U = T - T_m$ is the difference of the absolute temperature T and the equilibrium melting temperature T_m of the bulk. It is assumed that all the material parameters are independent of temperature, and that the densities of the solid and liquid are identical. Standard Dirichlet or Neumann conditions are imposed at the external boundaries. At points on the solid–liquid interface, conservation of heat requires that

$$L\mathbf{v} \cdot \hat{\mathbf{n}} = (\mathbf{Q}_L - \mathbf{Q}_S) \cdot \hat{\mathbf{n}}, \tag{2}$$

where L is the latent heat of fusion, $\mathbf{v}$ the velocity, $\hat{\mathbf{n}}$ the unit normal to the interface, and $\mathbf{Q}_L$ and $\mathbf{Q}_S$ the heat fluxes in the liquid and solid. The heat fluxes are $\mathbf{Q}_i = -K_i \nabla u$, where K_i is the thermal conductivity. The thermal diffusivities are related to K_i by $D_i = K_i / C_i$, where C_i is the heat capacity per unit volume. It assumed that the interface is in local thermodynamic equilibrium, so that movement of the interface is controlled by heat transport rather than by the kinetics of molecular attachment. In such conditions, the interface is rough on a molecular scale (crystalline facets do not form) and the temperature of a point on the interface obeys the Gibbs–Thomson relation

$$U = -\Gamma \mathscr{K}, \tag{3}$$

where Γ is a constant and $\mathscr{K}$ is the local curvature, taken to be positive if the interface is concave toward the solid. Γ is related to the surface tension γ by $\Gamma = \gamma T_m / L$. The effects of crystalline anisotropy are ignored, so that γ is independent of direction.

When the temperature of the liquid is greater than the equilibrium melting temperature, the interface is stable in the sense that small perturbations of its shape are damped out. As a result, the motion and shape of the interface conform to the geometry of the large-scale heat flow. In this case, Eq. (3) plays a very minor role. When the liquid is supercooled, however, it is possible for the interface shape to become unstable and develop a small-scale structure that is essentially independent to the overall heat flow. The surface tension plays a crucial role in this process, via Eq. (3), because it acts to stabilize the interface against short-wavelength perturbations. A planar interface, for example, first goes unstable at a characteristic wavelength which is approximately equal to the geometric mean $\sqrt{d_0 l}$ of the capillary length d_0 and the thermal diffusion length l [4]. Typically d_0 is of the order of angstroms, l is of the order of centimeters, and the initial instability and the complex patterns that evolve from it are of the order of microns.

The basic mechanism of the instability and the restabilization provided by the

surface tension are easy to understand. Consider the unstable steady-state situation shown in Fig. 1a, where a planar interface is advancing to the right. The interface and the solid behind it are at the melting temperature, $U = 0$, while the liquid far to the right is held at a temperature $U = -1$. The velocity of the interface is proportional to the steepness of the temperature profile in the adjacent liquid (Fig. 1b). In the absence of surface tension, a small protrusion on the surface of the solid, as in Fig. 1c, will grow faster than the surrounding plane interface because the temperature profile near it is steeper. Surface tension reduces the temperature at the tip of the protrusion below T_m, as shown in Fig. 1d, which flattens the temperature profile and also allows a flow of heat toward the interface in the solid. The greater the curvature, the more the velocity is reduced. In the absense of surface tension, the area within a depression in the solid, as in Fig. 1e, grows more slowly than the plane, and is left further and further behind. Here the effect of surface tension is to raise the interface temperature above T_m, as shown in Fig. 1f, thereby increasing the flow of heat away from the interface and accelerating the growth of solid there.

There are a number of factors that make a numerical solution of Eqs. (1)–(3) challenging. Heat conduction with a moving boundary is difficult to handle, especially in two or more dimensions, even when the surface tension is ignored and there is no supercooling. Work on the numerical solution of such problems is an area of active research [5]. Additional difficulties are raised by the need to calculate the curvature, since the position of the interface must be determined accurately on a scale that is small compared to the thermal diffusion length. Furthermore, the coupling of the effect of the curvature to the temperature field requires that the features shown in Figs. 1b–1f, including the discontinuity of slope at the interface, are adequately represented.

Existing methods for the solution of the moving-boundary problem in the absence of surface tension may be grouped in two classes [6, 7]. First are front-tracking methods, where the location of the interface is explicitly calculated at each time step. The differential equation (1) is solved separately in each single-phase region, and the

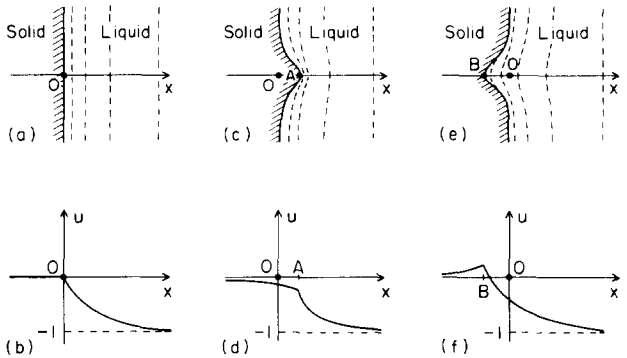

FIG. 1. Illustration of the effect of surface tension on the interface temperature. Top: interface shapes and isotherms. The solid is growing into the supercooled liquid. Bottom: the corresponding temperature profiles along the x-axis.

boundary condition (2) is applied at the interface. Second are the single-domain methods, where Eqs. (1) and (2) are transformed to an equation which applies in the whole domain. In these methods, which are also known as the enthalpy or weak-formulation methods, the explicit location of the interface is not required in the calculation. The method used in this paper, described in detail in the next section, contains features of both approaches. It is based on a weak formulation of the problem over the whole domain, but because of the need to calculate the curvature and to approximate the temperature profile in fine detail near the interface, the position of the interface is explicitly represented. Results of the application of the method to a model problem are presented in Section III. In the final section, some limitations of the method are discussed, and plans for future work are indicated.

II. Method

The single-domain formulation of the moving boundary problem is obtained as follows. Both the diffusion equation (1) and the interface boundary condition (2) are consequences of the conservation of heat, and can be derived from an integral form of the conservation law which is valid over the entire domain of the problem. The equation involves the enthalpy function H defined as

$$H = \begin{cases} C_L U, & \text{liquid phase} \\ C_S U - L, & \text{solid phase.} \end{cases} \tag{4}$$

H is shown schematically in Fig. 2a. Solid lines indicate the branches of the curve

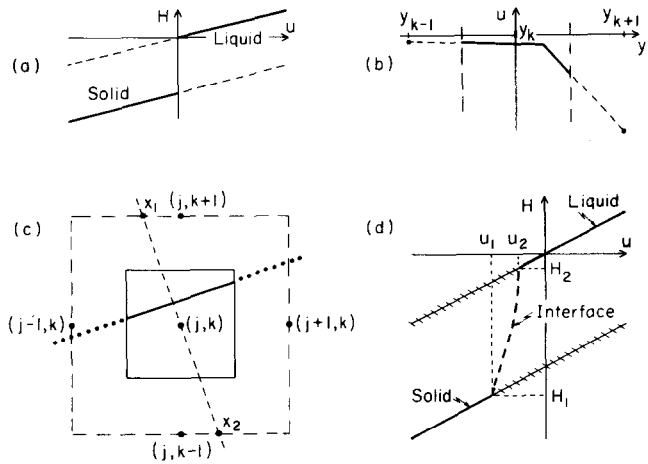

FIG. 2. (a) Enthalpy vs temperature. Solid lines indicate the equilibrium phases, dashed lines the metastable ones. (b) Temperature profile in an interface cell with the interface parallel to the x-axis. (c) Construction to determine the extrapolation points $\mathbf{x}_1, \mathbf{x}_2$. The extension of the interface line into neighboring cells, dotted line, is used in determining the directional effective temperatures. (d) Enthalpy function determined by the piecewise linear temperature field for a typical interface cell. The cross-hatched parts of the normal H versus U lines are inaccessible.

correponding to the equilibrium phases, and dotted lines indicate the metastable branches. In problems where superheating and supercooling do not occur, H is a single-valued function of U, and for computational convenience a segment of large slope joining the equilibrium solid and liquid branches is often introduced. Such a strategem is not possible here, and H must be treated as an explicit function of the phase as well as of U.

The integral conservation law is

$$\int_{\mathscr{S}} \{Hn_t - \mathbf{Q} \cdot \mathbf{n}_x\}\, dS = 0, \tag{5}$$

where $\mathscr{S}$ is any closed surface in space–time, n_t is the time component, $\mathbf{n}_x$ is the space component of the unit outer normal $(\mathbf{n}_x, n_t)$ to $\mathscr{S}$, and $\mathbf{Q}$ is the heat current density. The diffusion equation (1) is recovered from (5) if one takes $\mathscr{S}$ to enclose a small volume which is entirely solid or liquid, integrates by parts, and then lets the volume shrink to zero. The boundary condition (2) is obtained if $\mathscr{S}$ is taken to enclose a small portion of the interface [8].

We now specialize to two spatial dimensions and introduce a uniform spatial grid with $x_{j+1} - x_j = \Delta x = y_{k+1} - y_k$ and a uniform grid in time with $t_{n+1} - t_n = \Delta t$. A grid point (jk) is regarded as lying in the center of the square grid cell with $|x - x_j| \leqslant \frac{1}{2}\Delta x$ and $|y - y_k| \leqslant \frac{1}{2}\Delta x$. Except for the phase function P_{jk}, functions on the spatial grid are defined as averages of the continuous function over a cell. Thus H^n_{jk} represents H evaluated at the nth time step and averaged over the jkth cell. The phase P^n_{jk} is defined to be solid or liquid if the jkth cell contains only that one phase at $t = t_n$, and to be interface if the cell contains both phases. The treatment of the interface cells is described in detail below.

The discrete form of the conservation law is obtained by applying (5) to the surface of the cube whose top and bottom are the jkth cell at times t_{n+1} and t_n. The contribution to the integral of the top and bottom is simply $(\Delta x)^2(H^{n+1}_{jk} - H^n_{jk})$. The integrals at the sides are taken to be averages of the integrals along the edges at each time step. For example, the integral over the surface at $x = x_j + \frac{1}{2}\Delta x$ is given by $\frac{1}{2}\Delta t(Q^{x,n+1}_{j+1/2,k} + Q^{x,n}_{j+1/2,k})$, where

$$Q^{x,m}_{j+1/2,k} = \int_{y_k - \Delta x/2}^{y_k + \Delta x/2} \hat{\mathbf{x}} \cdot \mathbf{Q}(x_j + \tfrac{1}{2}\Delta x, y, t_m)\, dy. \tag{6}$$

The conservation law can now be written

$$H^{n+1}_{jk} = H^n_{jk} + F^n_{jk} + F^{n+1}_{jk}, \tag{7}$$

where

$$F^m_{jk} = -\frac{\Delta t}{2(\Delta x)^2}(Q^{x,m}_{j+1/2,k} - Q^{x,m}_{j-1/2,k} + Q^{y,m}_{j,k+1/2} - Q^{y,m}_{j,k-1/2}). \tag{8}$$

The terms of Eq. (8) are simple to evaluate when the cell jk and its neighbors are all

either solid or liquid. In this case the finite difference approximation to $\mathbf{Q} = -K\,\nabla U$ gives, for example,

$$Q^{x,n}_{j+1/2,k} = -\tfrac{1}{2}(K^n_{jk} + K^n_{j+1,k})(U^n_{j+1,k} - U^n_{jk}). \tag{9}$$

Equation (7) is a nonlinear system which is to be solved for H^{n+1}_{jk}, and, implicitly, U^{n+1}_{jk} and P^{n+1}_{jk}, in terms of the values given at t_n.

The treatment of the interface cells will now be described. The basic idea is to approximate the temperature within an interface cell by a piecewise linear function, in the spirit of the finite-element method. The interface within the cell jk is approximated by a line segment having slope m and intercept b with respect to local coordinates $\bar{x}, \bar{y}$ which are scaled so that the boundaries of the cell are $\bar{x} = \pm\frac{1}{2}$, $\bar{y} = \pm\frac{1}{2}$. The temperature profile over the interface cell is approximated by two linear pieces, continuous at the interface line. Thus for the interface line $\bar{y} = m\bar{x} + b$, the temperature in the cell has the form

$$U = \begin{cases} U_I + a^{>}(m\bar{x} + b - \bar{y}), & y \geqslant m\bar{x} + b \\ U_I + a^{<}(m\bar{x} + b - \bar{y}), & y \leqslant m\bar{x} + b, \end{cases} \tag{10}$$

where U_I is the temperature at the interface line. For clarity of exposition, all examples will use this representation. In practice, cells with interface lines that would have $|m| > 1$ in this form are treated to a local coordinate transformation $\bar{x} \leftrightarrow \bar{y}$.

The coefficients $a^{>}$ for the upper U-plane and $a^{<}$ for the lower are fixed by the requirement that these planes intersect certain points determined by extrapolation from the temperatures of neighboring cells. Consider the cross section of the temperature profile shown in Fig. 2b, for a case where the interface is parallel to the x-axis ($m = 0$). Here each U-plane is drawn so that its extension into the neighboring cell has the temperature $U_{j,k\pm1}$ at the center. For the more general case, where $m \neq 0$, the extrapolation points $\mathbf{x}_1$ and $\mathbf{x}_2$ are given by the intersection of the line perpendicular to the interface that passes through the center of the cell, with the lines $\bar{x} = \pm 1$, $\bar{y} = \pm 1$ that connect the eight grid points nearest to the cell, as shown in Fig. 2c. For $|m| \leqslant 1$, these points are $(-m, 1)$ and $(m, -1)$ in the local coordinates. The temperatures at these points are determined by linear extrapolation from the two nearest grid points.

The slope of the interface line is set equal to the slope of the line connecting the midpoints of the two nearest interface lines on either side. The position of the interface line within the cell is not directly fixed by the neighbors, however. Rather, the value of the intercept b is determined by the solution to the conservation law (7) for the cell. This is discussed in detail below. Once b is known, the curvature $\mathscr{K}$ of the interface is calculated by finding the circle which passes through the midpoints of the interface line and its two nearest neighbors. The magnitude of $\mathscr{K}$ is equal to the inverse of the radius of the circle, and its sign is determined from the location of the center of the circle according to the rule given in the introduction. The interface temperature is then given by Eq. (3).

The remaining quantities needed in the calculation are determined by the temperature profile. An expression for the enthalpy H_{jk} in terms of m, b, $a^<$, and $a^>$ is obtained by integrating Eq. (4), with U given by Eq. (10), over the cell. The heat flux terms in Eq. (8) could be obtained directly from their definitions, Eq. (6), etc., in the same way. However, a simpler approximation is used here: each interface cell is assigned a direction-dependent effective temperature, obtained from Eq. (10) by setting $\bar{x} = \bar{y} = 0$. Whether the value for the upper or lower region is used depends on the location of the interface line. In the situation depicted in Fig. 2c, for example, the neighboring grid points $j-1, k$ and $j, k+1$ lie above the extension of the interface line, so the temperature derived from the upper U-plane of the jk cell is used for those directions. The heat fluxes are then given by Eq. (9), etc., with the appropriate directional temperature substituted for U^n_{jk}.

The conservation law (7) together with the relations just described for the interface cell quantities form a complicated system which is solved by iteration. During a sweep through the grid, all quantities are recalculated for each cell on the basis of the current neighboring cell values, except for the slopes m and temperatures U_I of the interface lines; these are recalculated separately after each complete iteration cycle. Consider now the jkth cell during an iteration cycle. All quantities at the last time step are known, all quantities involving neighboring cells at the current time step are considered known (some of these are values calculated during the present iteration, others during the previous one), and if the jkth cell was an interface cell during the last iteration, the slope and temperature of the interface line are known. The task is to solve for H_{jk}, U_{jk}, and P_{jk}; if $P_{jk} =$ interface, this requires solving for the position b of the interface line.

For simplicity, the following discussion assumes that the thermal conductivities of solid and liquid are identical. There is no essential change when $K_S \neq K_L$, but then a number of different cases depending on the phases of the cell and its neighbors via Eq. (9), etc., must be specified. Let P and U be the values of the phase and temperature to be found for the cell jk in the present iteration. For an interface cell, the temperature is $U = U_S + U_L$, where U_S and U_L are the results of integrating the U-profile over the parts of the cell that are solid and liquid, respectively; they are functions of the unknown interface position b. Let A_S be the fraction of the area of an interface cell that is occupied by solid. Now the conservation law (7) can be written

$$C_S U - L = G - \sigma U, \qquad \text{if } P = \text{solid} \tag{11a}$$

$$C_S U_S + C_L U_L - L A_S = G - \sigma(U_S + U_L), \qquad \text{if } P = \text{interface} \tag{11b}$$

$$C_L U = G - \sigma U, \qquad \text{if } P = \text{liquid}, \tag{11c}$$

where G is the sum of all terms on the right-hand side of (7) that do not explicitly contain $U = U^{n+1}_{jk}$, and σ is $K(\Delta t)(\Delta x)^{-2}$. Equations (11a) and (11c) can be solved for U immediately, but (11b) is a nonlinear equation for b. Of course, the phase P remains to be determined.

It is important to note here that the interface is not constrained to be continuous

from one cell to next, nor is there required to be an interface cell separating solid and liquid cells. However, there is an essential constraint on the phase of a cell: for a cell to be an interface cell it is required that at least one of its nearest neighbors be solid and at least one be liquid. This neighboring-cell condition is the simplest way of implementing the physical requirement for heterogeneous nucleation—i.e., solid forms only on preexisting solid—without which the persistence of the metastable phases would be impossible.

The solution of Eqs. (11) depends first of all on the phase of the cell at the last iteration and on the current phases of its neighbors. If the cell was solid or liquid at the last iteration and it does not satisfy the neighboring-cell requirement for an interface cell, then the phase remains unchanged and Eq. (11a) or (11c) is solved for U. The new temperature of the cell is then taken to be

$$U^i = \phi U + (1 - \phi)\, U^{i-1}, \tag{12}$$

where U^{i-1} is the value of the temperature of the cell at the previous iteration and ϕ is an overrelaxation parameter. If the cell does satisfy the neighboring-cell requirement, or if it was an interface cell at the last iteration, the new phase and temperature are determined from Eqs. (11) as follows.

Figure 2d shows the three branches of H (solid, interface, and liquid) as they appear on the left-hand sides of Eqs. (11). Let b_S be the value of b for which $A_S = 1$, and b_L the value for which $A_S = 0$. Clearly, if G is large enough so that $G - \sigma U$ is greater than the maximum value H_2 of the interface branch for all values of b, then the phase of the cell is liquid and the temperature is obtained from Eq. (11c). Likewise if G is sufficiently small, the phase is solid. Let us define

$$W(b) = (c_S + \sigma)\, U_S + (c_L + \sigma)\, U_L - LA_S - G \tag{13}$$

so that the equation $W(b) = 0$ is equivalent to Eq. (11b). Then the solution of the conservation law is $P =$ solid and $U^i = (G + L)/(c_s + \sigma)$ if $W(b_s) > 0$, $P =$ liquid and $U^i = G/(c_L + \sigma)$ if $W(b_L) < 0$, and $P =$ interface with b determined by $W(b) = 0$ otherwise. It should be noted that if P is interface, the solution to $W(b) = 0$ is guaranteed to be in the range $\min(b_s, b_L) \leqslant b \leqslant \max(b_s, b_L)$.

In summary, the overall structure of the calculation is as follows. Starting with complete information about the nth time step, one sweeps through the grid, solving the conservation law for P^i and U^i at the $(n + 1)$st time step for each cell, and for b for each interface cell. At the end of each iteration, the slopes m and the temperatures U_I for each interface cell are recalculated. The process is then repeated until the convergence criterion $\max |U^i - U^{i-1}| \leqslant \varepsilon$ is satisfied.

III. Results

Figure 3 shows the development of an interface pattern that mimics dendritic growth. In this example, the calculation is started from a single grid–cell seed of solid at $U = 0$ in a background of uniformly supercooled liquid at $U = -1$. The fourfold

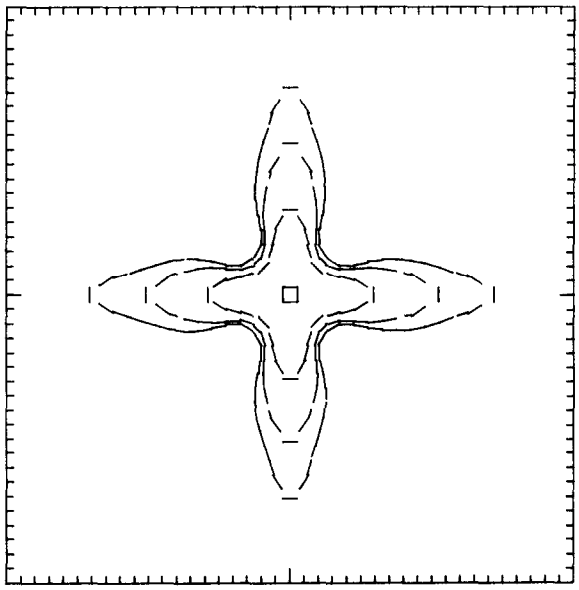

FIG. 3. Dendrite-like growth developed from a single grid–cell seed of solid in a background of uniformly supercooled liquid. The interface curve is shown at equal time intervals. The fourfold symmetry of the pattern is determined by a grid-dependent effect of the initial seeding.

symmetry of this pattern is determined by the grid, because of the initial seeding. With larger values of the surface tension, however, the four-armed shape that develops from the same initial seeding quickly restabilizes and grows as a circle.

To test the method quantitatively, I have applied it to a simple problem where the results can be compared with an approximate analytical solution. The problem is the two-dimensional growth and stability of a cylinder of solid with radius R surrounded by supercooled liquid in a cylindrical container with fixed temperature $U = -1$ at the wall. The radius of the container is R_c. For simplicity, it is assumed that $K_S = K_L = K$ and $C_S = C_L = C$. We wish to solve for the velocity at which the radius of the cylindrical solid grows and for the exponential amplification rate of small perturbations. For the conditions we consider, the interface moves very little in the time required for relaxation of the temperature field, and the time derivative can be dropped from Eq. (1). In this quasistationary approximation, the growth velocity of the circular cylinder of radius R_0 is found to be

$$v = \frac{K(1 - \Gamma/R_0)}{LR_0 \ln(R_c/R_0)} \tag{14}$$

and the temperature field to be

$$U(r) = \begin{cases} -\Gamma/R_0 + \alpha \ln(r/R_0), & r \geqslant R_0 \\ -\Gamma/R_0, & r < R_0, \end{cases} \tag{15}$$

where $\alpha = (\Gamma/R_0 - 1)/\ln(R_c/R_0)$.

Column I of Table I gives the results of the numerical calculations of the radial velocity of a circular interface. The calculations are done on a square grid with n_p grid points on a side. The length of the side of the square is taken to be unity, so the grid spacing Δx is $(n_p - 1)^{-1}$. To approximate an outer boundary circle with $R_c = 0.5$, grid points at a distance 0.5 or greater from the center are held at the temperature $U_c = -1$. All the calculations of Table I were done with $C_L = C_S = K_L = K_S = 1$ and $L = 2$. The calculations of column I used $\Gamma = 0.01$. Figure 4 shows the interface at time intervals of 0.005, starting with $R_0 = 0.15$, for the calculation with $n_p = 61$. The velocity is obtained by a least-squares fit of the mean radius vs time over the interval $t = 0.005$ to 0.025. The calculated values are in excellent agreement with the predicted velocity in the quasistationary approximation, Eq. (14), which is nearly constant at 2.57 for R_0 in that range. The consistency of the calculation even for the coarsest grid used is impressive. Also noteworthy is the degree to which circularity is maintained, as seen in Fig. 4; the deviation from the mean radius is always less than 0.3% in this example. The applicability of the quasistationary approximation here is verified by the observation that the calculated temperature field is essentially indistinguishable from Eq. (15) at the same R_0.

Because Eqs. (7) and (8) provide a fully implicit solution of the heat diffusion problem in the absence of the special approximation for the temperature profile of the interface cells [9], it was hoped that in spite of the nonlinearities in the problem, the procedure developed here would likewise be free of the well-known limitation of explicit methods to time steps proportional to the square of the grid spacing. It was found, however, that large time steps sometimes led to convergence problems and obviously erroneous results, so the calculations reported here were done with time steps smaller than $\frac{1}{2}(\Delta x)^2$, as indicated in Table I. Typically 10 to 15 iterations are

TABLE I

Calculated Velocity v of Circular Growth and Amplification Rates ω_m of the Perturbation are Compared with the Predictions of the Quasistationary Approximation

n_p	Δt	I v	II ω_2	III ω_2	IV ω_3	V ω_4	VI ω_4
21	1.0×10^{-3}	2.62	10.2	11.1	22.4	—	—
31	5.0×10^{-4}	2.58	10.9	13.8	21.8	26.4	33.2
41	2.5×10^{-4}	2.54	10.2	13.9	21.1	33.0	30.3
61	1.25×10^{-4}	2.54	9.8	12.6	20.3	33.6	26.2
Quasistationary		2.57	9.5	9.5	19.8	30.6	30.6
	Γ	0.01	0.005	0.005	0.002	0.001	0.001
	R_0 range	0.15–0.21	0.20–0.26	0.20–0.26	0.23–0.29	0.23–0.29	0.23–0.29
	θ_0	—	0	$\pi/4$	0	0	$\pi/4$

Note. Values of n_p, Δt, Γ, R_0, and θ_0 used in each calculation are also shown.

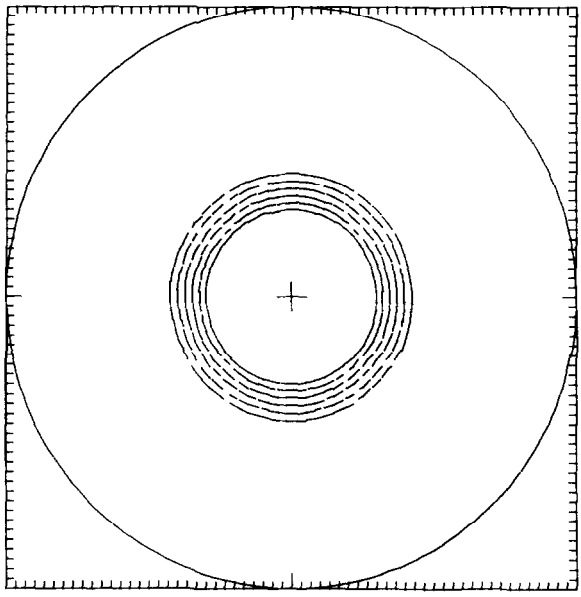

FIG. 4. Interface surve at equal time intervals showing the growth of the solid (interior) in the stable circular mode.

required for convergence. For $n_p = 61$, one time step takes approximately 6 sec of DEC-2060 CPU time.

A solution can also be obtained in the quasistationary approximation for surfaces of the form

$$R(t) = R_0(t) + A_m e^{\omega_m t} \cos(m(\theta - \theta_0)) \tag{16}$$

with $m = 2, 3, 4, \ldots$. To first order in the perturbation, the exponential growth rate is

$$\omega_m = \frac{(m-1)v}{R_0}\left[1 - \frac{2K\Gamma m(m+1)}{vLR_0^2}\right] \tag{17}$$

and the temperature field is

$$U(r,\theta,t) = \begin{cases} -\left(\dfrac{\Gamma}{R_0}\right) + \alpha \ln \dfrac{r}{R_0} - A_m\left(\dfrac{\alpha}{R_0} + \beta\right)\left(\dfrac{R_0}{r}\right)^m \cos(m(\theta - \theta_0)), & r \geqslant R(t) \\ -\left(\dfrac{\Gamma}{R_0}\right) - A_m\beta\left(\dfrac{r}{R_0}\right)^m \cos(m(\theta - \theta_0)), & r < R(t), \end{cases} \tag{18}$$

where α is the same as in Eq. (15) and $\beta = \Gamma(m^2 - 1)/R_0^2$.

The numerical calculations were done using Eqs. (16) and (18) for the initial state at $t = 0$. Columns II–VI of Table I give the results for calculations of ω_m for $m = 2, 3$, and 4. Values of Γ were chosen for each m so that the quasistationary

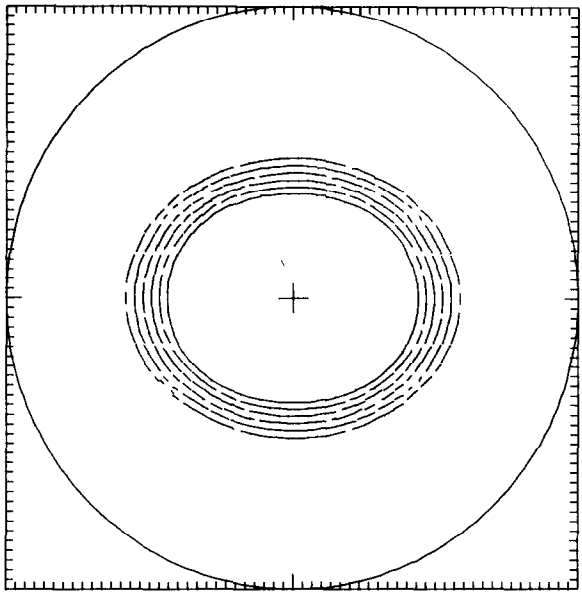

FIG. 5. Interface curve at equal time intervals starting from a perturbed circle with $m = 2$ and $\theta_0 = 0$.

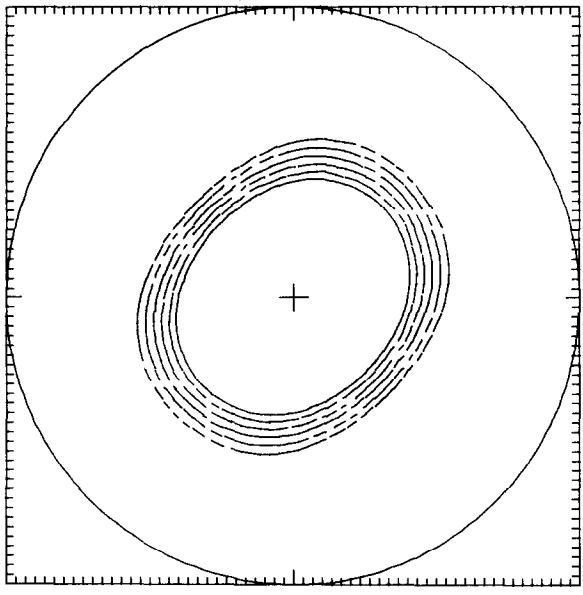

FIG. 6. Same as Fig. 5 but with the long axis of the initial curve oriented at 45° to the grid axes.

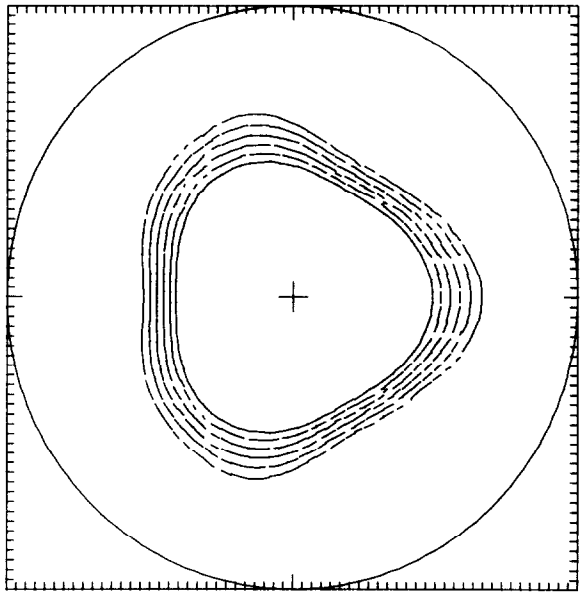

FIG. 7. Interface curve at equal time intervals for the $m = 3$ perturbation. A distortion of the shape due to direction-dependent effects of the grid is visible at the later times.

approximation for ω_m is nearly constant over the range of R_0 used. The growth rates were obtained by fitting the calculated interface positions to a curve of the form (16) and then fitting the amplitudes to an exponential function in time. The calculations in columns II and III for $m = 2$ and columns V and VI for $m = 4$ differ only in the parameter θ_0, which gives the orientation of the perturbation with respect to the grid. Figures 5 and 6 show the interface curve at time intervals of 0.005 for the $\theta_0 = 0$ and $\theta_0 = \pi/4$ cases, respectively. In all cases an initial amplitude of 10% R_0 is used. Calculations done with initial amplitudes of 5–15% show a scatter of about 10% in each ω_m, with no observable amplitude dependence.

Most of the computed ω_m agree with the quasistationary approximation within their estimated accuracy of about 10%. The values calculated for these small-amplitude quantities are not expected to be as good as for the growth velocity of the unperturbed circle, of course. The results are also more sensitive to directional effects of the grid, as shown by the dependence on the angle θ_0, and by the slight distortion in the shape of the $m = 3$ interface seen in Fig. 7. This is discussed in the next section.

IV. DISCUSSION

This paper reports a new method for studying shape instabilities in solidification by direct numerical solution of the moving boundary problem. The results are in

excellent agreement with the predictions of the quasistationary approximation for a model problem. The basic idea of the method is the approximation of the temperature field in an interface cell by a piecewise linear function, in the spirit of the finite-element technique. The following discussion points out areas of difficulty with the present implementation of the idea and indicates some possible directions for future work.

There are a number of obvious changes that could be made to improve the speed and accuracy of the present program. For example, the local curvature is now calculated using only three points to define a circular arc. When an interface line segment is nearly horizontal or nearly vertical and intersects two adjacent edges of the cell, the location of its midpoint can change very rapidly with small changes in b, which leads in turn to large changes in the curvature and sometimes prevents convergence. To handle this, the curvature calculated for each interface cell at the end of an iteration is averaged with the previous values, and furthermore the value of the curvature is frozen after a number of iterations. This ad hoc procedure is roughly satisfactory because the curvature in fact would change very little during a time step if not for such artifacts of the calculation. A better solution would be to obtain the curvature by local fitting of a smooth curve to the interface using more than three points.

Another convergence difficulty appears when the interface line is roughly at 45° to the grid axes and very close to the corner of a cell. In this situation, the W function, Eq. (13), may be nearly independent of b locally, so that relatively large changes in b occur in successive iteration steps. The result can be a phase oscillation in which, for example, a cell alternates between being interface with $A_s = 0.98$ and being solid. The changes in the enthalpy and the temperature of the cell are very small, but the calculation of the curvature and the heat fluxes of the neighboring cells may be affected enough to prevent convergence. In the present program, this has been handled simply by cutting off all phase changes after a certain number of iterations within a time step. It has recently been learned [10] that the phase oscillations and the need for such a cutoff are eliminated if the heat fluxes are calculated by integration of the temperature profile of the cell, as mentioned in the third paragraph following Eq. (10).

It is crucial to the study of solidification patterns that the numerical method not introduce a directional bias, since the shape instability is inherently very sensitive to small differences in the interface position. The present program does remarkably well in maintaining an accurately circular shape when that is the stable mode. However, there is a small but significant directional bias in the grid, as shown by the approximately $\pm 10\%$ dependence of the $m = 2$ and $m = 4$ amplification rates on θ_0. The major source of the directional effect is easy to identify: the nearest-neighbor conditions for an interface cell make it impossible for portions of the interface curve that are not parallel to the grid axes always to be represented as a continuous sequence of line segments. This is especially true when the interface runs at approximately 45° to the grid, as can be seen in Fig. 4, for example. Preliminary work indicates that it is possible to solve this problem by generalizing the neighboring-cell

conditions so that a continuous interface is maintained at all angles [10]. The new condition allows cells with next-nearest neighbors of liquid and solid to be interface cells also, provided that they have two adjacent nearest-neighbor interface cells with interface lines at appropriate positions and orientations. The latter requirement appears to be necessary to make the choice of interface cells unique and independent of the iteration process.

The present version of the program has not been optimized for speed, and there are opportunities for considerable improvement by straightforward programming changes. However, the limitation to time steps proportional to $(\Delta x)^2$ appears to be a more fundamental problem. Perhaps the limitation can be eliminated by the improvements in the curvature and the neighboring-cell conditions mentioned above, or by changes in the iteration procedure. It is possible, on the other hand, that the basic time integration scheme, which is unconditionally stable for linear problems, could have intrinsic instabilities in this nonlinear problem. I suspect, however, that the small time-step requirement is due to the procedure which allows the interface position in each cell to be adjusted independently. The other problems discussed here also stem basically from the potential lack of continuity of the interface from cell to cell. For example, the need for cell-based nucleation conditions would disappear if the interface were guaranteed to be continuous at all times.

It is attractive, therefore, to propose to construct a method in which both the interface and the temperature field throughout the domain are approximated by continuous piecewise polynomials, as a natural extension of the finite-element idea in the moving boundary problem. Because of the role of the curvature in the instability problem, higher-order elements with curved boundaries at the interface might have a special advantage over linear elements. If the interface position were adjusted in a locally concerted way, rather than one mesh point or one element at a time, the short time-step limitation might be circumvented. Finally, this complete finite-element approach would probably be more susceptible than the present method to analysis and proof of convergence properties.

ACKNOWLEDGMENTS

This research was initiated and carried out under the direction of James Langer, to whom I offer my warmest thanks for his vision and support. George Fix and Robert Sekerka also contributed suggestions and comments on a regular basis. The calculations utilized a DEC-20 computer at the Carnegie-Mellon University Computation Center and the computer-graphics facilities of the Center for the Joining of Materials. Support from the Materials Research Laboratory Section, Division of Materials Research, National Science Foundation, under Grant No. DMR 76-81561, and from the Air Force Office of Scientific Research, under Contract F44620-76-C-0103, is gratefully acknowledged.

REFERENCES

1. J. S. LANGER, *Rev. Modern Phys.* **52** (1980), 1.
2. W. W. MULLINS AND R. F. SEKERKA, *J. Appl. Phys.* **34** (1963), 323; **35** (1964), 444.

3. J. S. LANGER AND H. MÜLLER-KRUMBHAAR, *Acta Metall.* **26** (1978), 1681, 1689, 1697.
4. J. S. LANGER AND L. A. TURSKI, *Acta Metall.* **25** (1977), 1113.
5. "Moving Boundary Problems" (D. G. Wilson, A. D. Soloman, and P. T. Boggs, Eds.), Academic Press, New York, 1978.
6. G. H. MEYER, *in* "Moving Boundary Problems" (D. G. Wilson, A. D. Soloman, and P. T. Boggs, Eds.), p. 73, Academic Press, New York, 1978.
7. N. SHAMSUNDAR, *in* "Moving Boundary Problems" (D. G. Wilson, A. D. Soloman, and P. T. Boggs, Eds.), p. 165, Academic Press, New York, 1978.
8. G. J. FIX, *in* "Moving Boundary Problems" (D. G. Wilson, A. D. Soloman, and P. T. Boggs, Eds.), p. 109, Academic Press, New York, 1978.
9. G. H. MEYER, *SIAM J. Numer. Anal.* **10** (1973), 522.
10. R. MATHUR AND J. B. SMITH, unpublished.